Tectonophysics, 180 (1990) 87–100
Elsevier Science Publishers B.V., Amsterdam – Printed in The Netherlands

Structure and paleostresses in the Gilboa' region, western margins of the central Dead Sea rift

Yossef Hatzor [a]* and Ze'ev Reches [b]

[a] *Geological Survey of Israel, Jerusalem, and Department of Geology, Hebrew University, Jerusalem (Israel)*
[b] *Department of Geology, Hebrew University, Jerusalem (Israel)*

(Revised version accepted June 1, 1989)

ABSTRACT

Hatzor, Y. and Reches, Z., 1990. Structure and paleostresses in the Gilboa' region, western margins of the central Dead Sea rift. In: R.L. Kovach and Z. Ben-Avraham (Editors), Geologic and Tectonic Processes of the Dead Sea Rift Zone. *Tectonophysics*, 180: 87–100.

The relationships between tectonic paleostresses and major fault systems are analyzed for the Gilboa' region. The Gilboa' is a folded block on the western margins of the Dead Sea transform which has been deformed and uplifted at least since the Miocene. The tectonic paleostresses in the Gilboa' were determined by inversion of slip striations along small faults measured in the field and from the trends of basaltic dikes. One state of stress dominated the Gilboa' region since the Miocene; the principal axes of the calculated stress tensor are: σ_1 at 0°/122°, σ_2 vertical and σ_3 at 0°/032°. This stress fits well with the trends of the Syrian Arc folds in the Gilboa' and its is compatible with the observed normal slip along the Gilboa' fault. However, this stress is incompatible with the either left-lateral slip or normal faulting along the Dead Sea system. Possible mechanisms to resolve this incompatibility are discussed.

Introduction

The relationships between tectonic stresses and the sense of slip along large faults are frequently obscure or enigmatic (e.g., Zoback et al., 1987). Stress–fault relationships may indicate that contemporaneous structures are incompatible with respect to each other. These stress–fault relationships may be resolved when the tectonic stresses are determined in methods which are independent of the large faults. We present here such an analysis for the Gilboa' block in northern Israel. This block is located at the intersection between the Dead Sea transform and the Carmel–Gilboa' system of normal faults. The Dead Sea and Carmel–Gilboa' fault systems apparently require different stress regimes, and our objective is to resolve the time and stress relationships between them.

The Gilboa' block is about 20 km by 20 km in size and is located on the western margins of the N–S Dead Sea transform (Fig. 1). The exposed rocks are Late Cretaceous to Recent in age. Three tectonic elements dominate the Gilboa' block (Hatzor, 1988): The first is the Syrian Arc system developed along the northern margins of the Arabian Shield. This is a belt of open folds, monoclines, reverse faults and wrench faults. The second element is the Dead Sea transform, the boundary between the Sinai–Israel subplate and the Arabian plate. It is 1000 km long and trends in a general N–S direction from the Red Sea to the Taurus–Zagros Mountains. The Dead Sea system is a left-lateral, leaky transform (Garfunkel, 1981). The third element is the NW–SE extensional sys-

* Present address: Department of Civil Engineering, University of California, Berkeley, CA (U.S.A.)

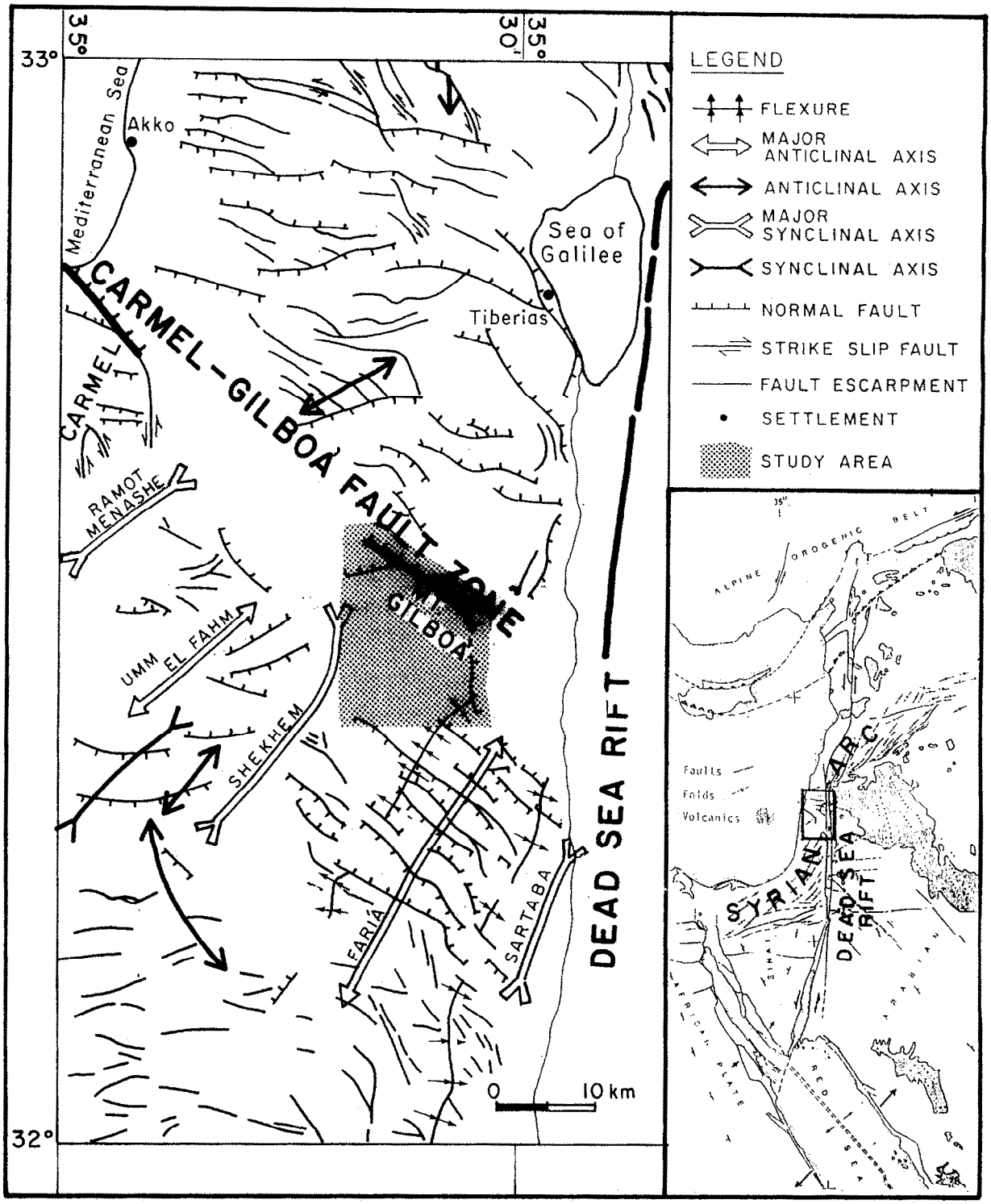

Fig. 1. Generalized tectonic map of northern Israel.

tem of the Carmel–Gilboa' zone which is part of a regional trend of normal faults and associated basaltic intrusions. The Gilboa' block is uplifted between the two bounding fault systems of the Dead Sea transform and the normal fault system of Carmel–Gilboa' (Fig. 1).

We analyze here the mechanical relationships between the regional fault system and the internal structure and paleostresses of the Gilboa'. First, the regional and local structure of the Gilboa' are described. Then, we determine the tectonic paleostresses and their ages by the analysis of small and large structures and igneous bodies. Finally, the character of the mechanical conditions along the major fault systems is discussed.

Structure of the Gilboa' region

Regional tectonic setting

The tectonic elements which affected the Gilboa' region, the Syrian Arc, the Dead Sea transform and the Carmel–Gilboa' system (Fig. 1) have been discussed by several investigators. De Sitter (1962) suggested structural development in a few stages. The NW–SE Late Cretaceous to early Eocene compression folded the NE–SW trending folds of the Syrian Arc, and caused sinistral motion along the Dead Sea rift. Later, the E–W compression of Eocene to Neogene times uplifted the region and initiated sinistral motion along the NW–SE trending faults of the Carmel–Gilboa' system, and dextral motion along the NE–SW trending faults in the Lebanon. Freund (1965, 1970) discussed the regional deformation of the Levant in terms of the left-lateral slip along the Dead Sea transform. He further suggested that left-lateral motion along the Carmel–Gilboa' fault compensates part of the local overlap of the Arabian and the Sinai–Israel plates. Neev (1975) considered the NE-striking folds and the NW-trending extensional faulting as genetically interrelated, and formed due to NW-trending compression of the region at least since the Jurassic. He related the sinistral movement along the Dead Sea rift to the Late Oligocene opening of the Red Sea.

Ben-Avraham and Hall (1977), suggested a Late Paleozoic age for the formation of the NW-trending Carmel structure. Schulmann and Bartov (1978) distinguished between two groups of structural, sedimentary and morphological elements in the Dead Sea rift. The first group, which is related to the rift, is of Pleistocene age, whereas the second group, which is transected by the rift, is older. Garfunkel (1981) suggested that the Syrian Arc structures formed under prevailing NW–SE compression (and the corresponding NE–SW extension) during Late Cretaceous to early Cenozoic times. Later, the NE–SW extension became the prevailing stress and generated the younger NW-trending extensional structures of the Gulf of Suez, Red Sea and the Carmel–Gilboa' zone, as well as the Dead Sea transform during the late Cenozoic. Bartov et al. (1980) showed that the Dead Sea transform was activated after the NW-trending dikes and faults of the Early Miocene had already developed.

Local structure of the Gilboa' block

The Gilboa' is an uplifted block about 20 km by 20 km in the northeastern corner of the Samaria mountains (Fig. 1). It is well defined on its northern and eastern margins by the Carmel–Gilboa' and Dead Sea faults, whereas on its southwestern side it is contiguous with the Samaria region (Figs. 1 and 2).

Folds

The Gilboa' block includes the large, western flexure of the Faria structure (Fig. 1) which comprises one open, gentle anticline and a minor syncline (Hatzor, 1988) (Fig. 2). The Faria is a 15 km wide box anticline, generated by two monoclinal flexures which trends N30°–40°E (Mimran, 1969) (Fig. 1). It is more than 30 km long and it plunges about 20° northward. This is the typical geometry of a Syrian Arc fold.

In agreement with other parts of the Syrian Arc, the erosional unconformity found in the northern Gilboa' based on folding initiated during the latter part of the Turonian. Folding continued during Cenomanian to Paleocene times, as inferred from stratigraphic thickness variations across the region (Hatzor, 1988). A folding phase during the early Eocene was recognized in the Gilboa' region (Hatzor, 1988) and south of it. Mimran (1984), who investigated the eastern flexure of the Faria structure south of the Gilboa', found Neogene sediments which are tilted to 37°, indicating post-Eocene deformation.

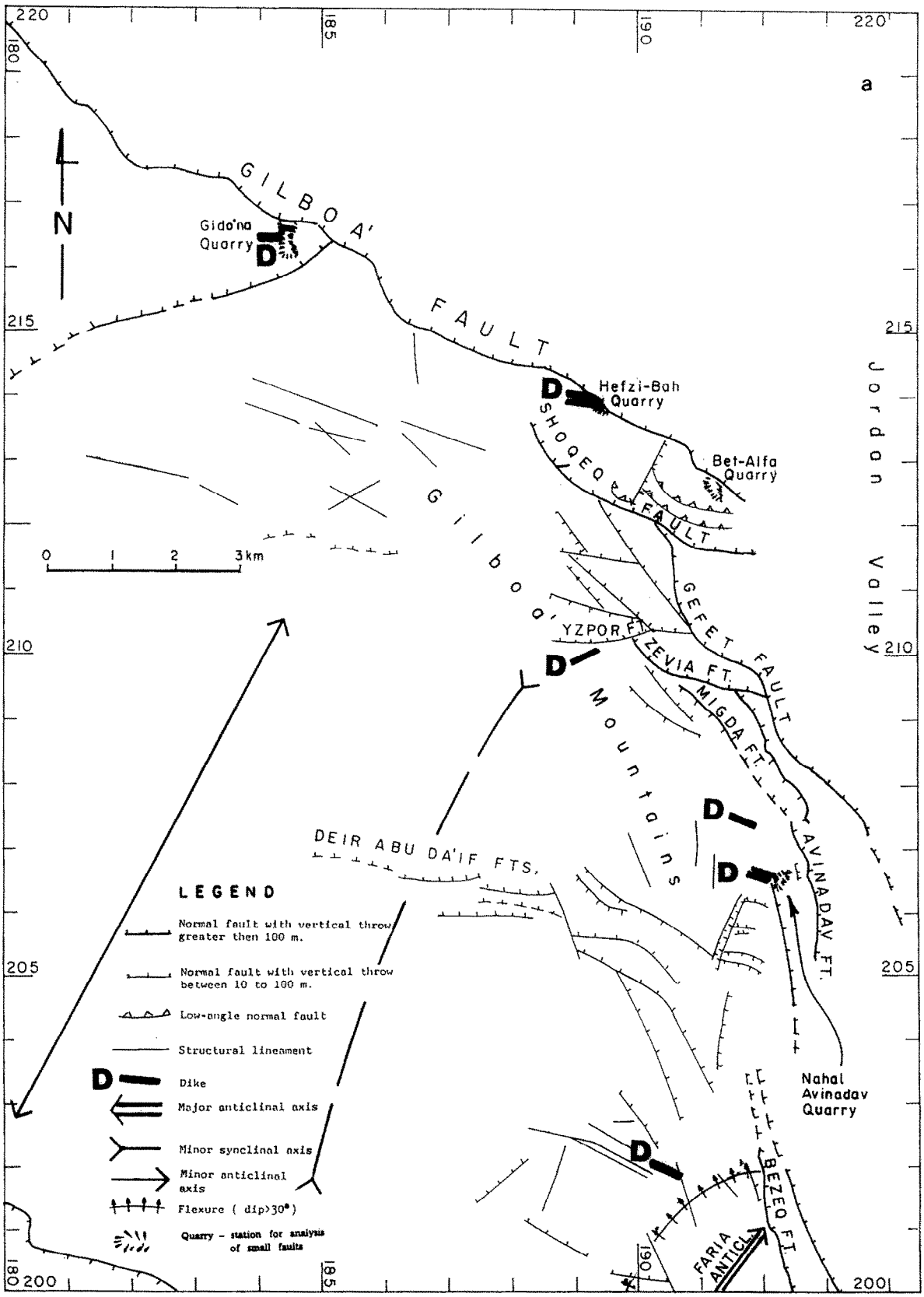

Fig. 2. Structural maps of the Gilboa' region. a. Structural elements. b. Structural contour map (after Hatzor, 1988).

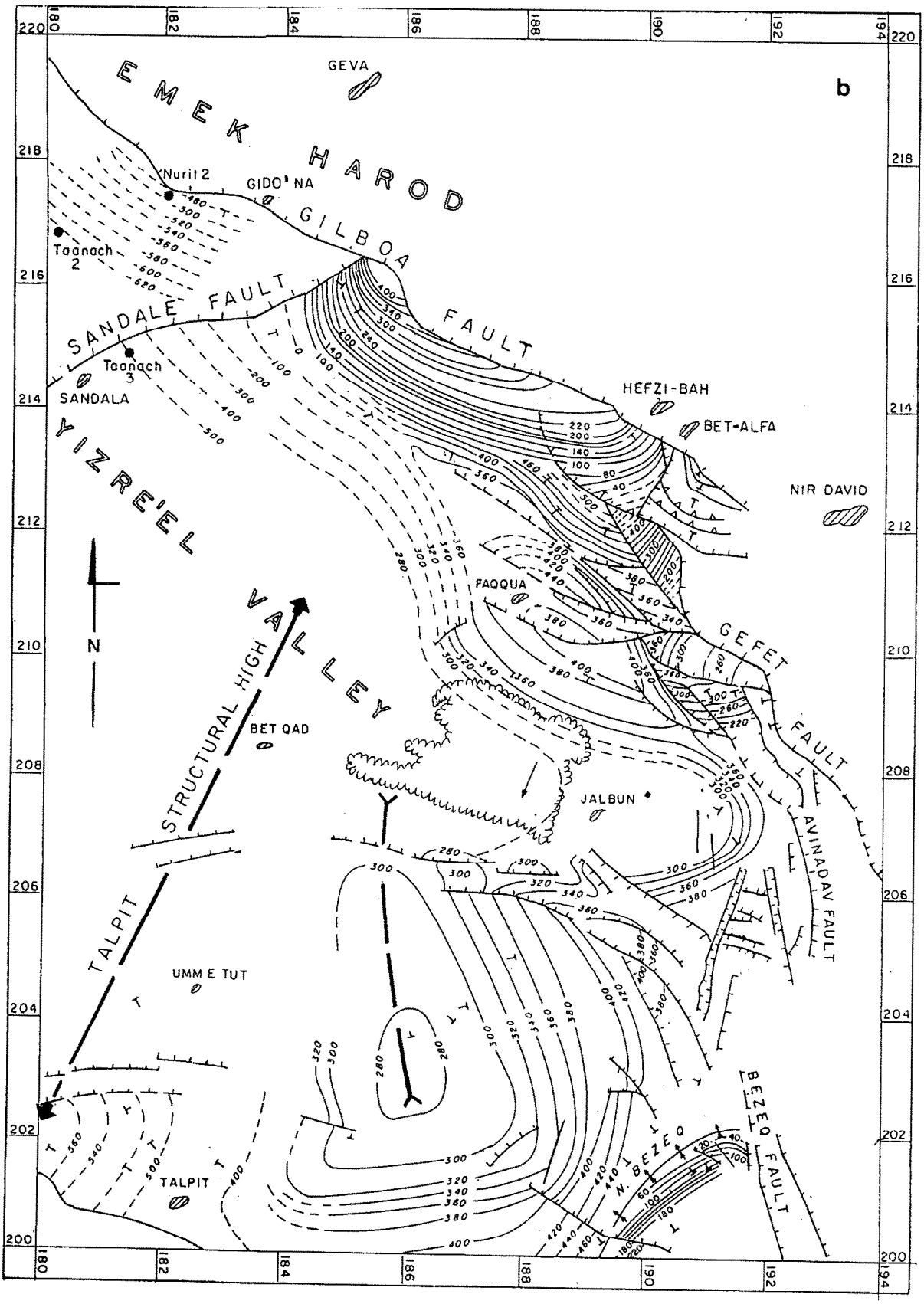

Fig. 2 (continued).

Faults

The northern and northeastern margins of the Gilboa' are intensively faulted by a system of en-echelon normal faults trending between west-northwest and northwest (Fig. 2). The faults form a zig-zag pattern, typical of normal faulting, which reflects the three-dimensional deformation (Reches, 1983). The maximum throw, along the Gilboa' fault which is the major fault in the system, is about 750 m; the throw along the other faults is up to 100 m. The NW-trending normal faulting post-dates a group of basaltic lavas, which are 15–17 Ma old, and continued after a younger group of basalts, which are 4.6–5.2 Ma old. These radiometric ages are according to Shaliv and Steinitz (1988).

The N–S trending faults of Dead Sea system cut the eastern margins of the Gilboa' (Fig. 2).

Analysis of the tectonic paleostresses

The tectonic paleostresses in the Gilboa' area were evaluated from measurements of small faults and their slip striations. The faults were measured in clusters of more then ten faults located at distances of up to 100 m from each other. Individual faults range in size from a few centimeters to a few tens of meters. We assume that the faults in each cluster were activated by a uniform state of stress. This stress was determined by the stress inversion method of Reches (1987), briefly described below.

We also use the orientations of Neogene dikes as indicators of the paleostress orientation, and apply the radiometric ages of these dikes to constrain the ages of the tectonic activity.

Measurement of small faults

Small faults were measured in three quarries along the margins of the Gilboa' (Fig. 2). All faults were measured for sense and direction of slip, as indicated by slickenside striations, fault surface irregularities, secondary mineralization and pressure-solution features. Normal, strike-slip and oblique faults were found. The measurements include 96 faults at five stations at the following locations (Fig. 2):

Gido'na quarry is located in the northwestern part of the study area, on the uplifted side of the Gilboa' fault. This is a quarry in the well-bedded lower to middle Eocene limestones (Hatzor, 1988). Layer thickness ranges from 10 cm to 2 m, with only a few shale layers present. The bedding surfaces are inclined at 12°–40° towards the north and north-northwest, roughly toward the Gilboa' fault. In this quarry, we measured 42 faults at three different sites separated from each other by 100–500 m. Thus, we regarded these sites as three separate stations. The uppermost station is the furthest from the Gilboa' fault (about 1000 m).

Bet-Alfa quarry is located in northeastern Gilboa' on the uplifted side of the Gilboa' fault like Gid'ona quarry, (Fig. 2). Bet-Alfa quarry is excavated in the lower to middle Eocene limestones and chalky limestones. Bedding surfaces are inclined at 26°–45° towards 015° to 045°, i.e., towards the Gilboa' fault. Bedding plane slippage is relatively common in this quarry, probably occurring due to the excavation and daylighting of the steep layers. Faults with clear slickenside striations are less common here then in Gido'na, and only twelve faults were measured at all levels in the quarry.

Nahal Avinadav quarry, where lower Eocene limestones are excavated, is located between two normal faults in the eastern part of the Gilboa' (Fig. 2). These faults are not the main faults of the Dead Sea rift, and their throw does not exceed 100 m. Bedding inclinations are consistent within the quarry, with a mean value of 8°/190°. The 37 faults with clear slickensides fall into two distinct groups: 20 faults of almost pure strike slip (Fig. 3e), and 17 faults of almost pure dip slip (Fig. 3f).

Stress inversion

The method

The stress inversion method of Reches (1987) calculates the stress state which can cause slip on a cluster of faults. It is based on the following assumptions:

(A) Slip on a fault occurs in the direction of maximum resolved shear stress (Bott, 1959).

(B) The shear and normal stresses on the fault satisfy the Coulomb yield condition of $\tau \geq C +$

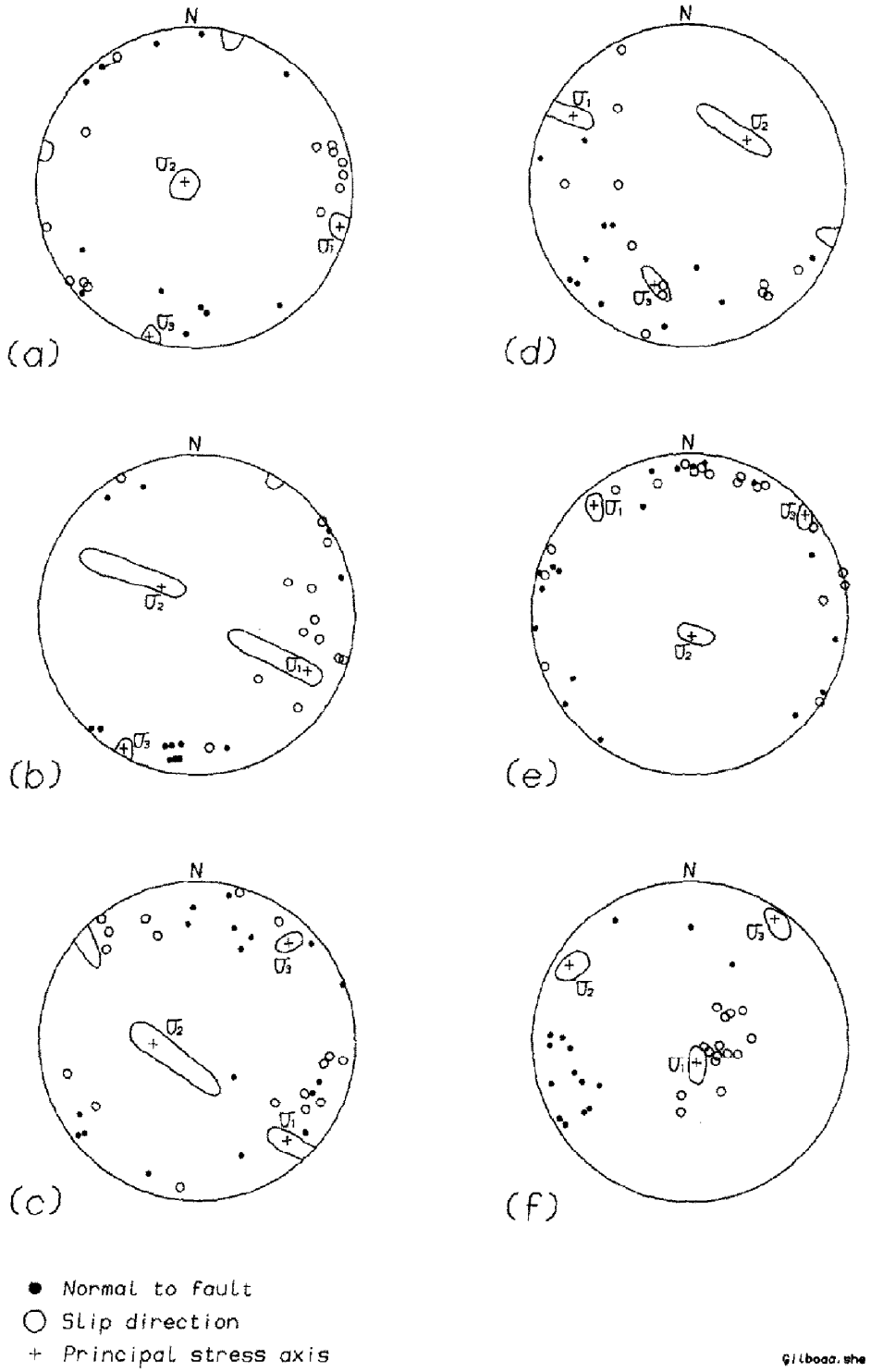

Fig. 3. Paleostress calculations in six fault clusters in the Gilboa' region. Lower hemisphere, equal-area projection; stress inversion after Reches (1987). The stereoplots include the poles to the measured small faults (dots), the measured slip axes (circles), and the best-fit stress tensor axes (marked σ_i) encircled with confidence margins of one standard deviation. Quarries are shown in Fig. 2. The clusters are as follows: a. Gido'na quarry, level 3. b. Gido'na quarry, level 4. c. Gido'na quarry, level 5. d. Bet-Alfa quarry. e. Nahal Avinadav quarry, strike-slip faults. f. Nahal Avinadav quarry, normal faults. See text and Table 1.

TABLE 1

Stress tensors calculated for fault clusters measured in the Gilboa'. Best-fit solutions (see text and Fig. 3); quarries in Fig. 2

Station	Number of faults	Mean friction [a]	Mean misfit angle [b]	Stress ratio [c]	Principal stress axes					
					Magnitudes [d]			Orientations [e]		
					σ_1	σ_2	σ_3	σ_1	σ_2	σ_3
a. Gid'ona 3	14	0.6	20.4	0.68	1.30	0.99	0.34	5/106	84/290	0/196
b. Gid'ona 4	13	0.3	20.5	0.54	1.25	0.95	0.61	22/116	67/307	3/208
c. Gid'ona 5	18	0.1	29.5	0.63	1.10	1.01	0.84	14/137	67/266	16/ 43
d. Bet-Alfa	12	0.2	26.2	0.42	1.35	1.05	0.83	15/301	51/ 51	34/200
e. Nahal Avinadav (strike-slip)	17	0.0	14.7	0.63	1.01	1.00	0.98	9/318	79/170	5/ 49
f. Nahal Avinadav (normal)	16	1.1	32.6	0.07	1.03	0.14	0.07	78/159	8/302	6/ 33

[a] Friction coefficient of the solution with the smallest misfit angle.
[b] Misfit of principal axes (Reches et al., 1989).
[c] $(\sigma_2 - \sigma_3)/(\sigma_1 - \sigma_3)$.
[d] Normalized by the effective overburden, $\sigma_v = 1.00$.
[e] Plunge (in degrees)/trend (in degrees from north).

$\mu\sigma_n$, where τ and σ_n are the magnitudes of the shear stress in the slip direction and the normal stress, C is cohesion, and μ is the coefficient of friction.

(C) In terms of the dimensions of the field station the slip events occurred under relatively uniform conditions.

Conditions (A) and (B) are formulated for each individual fault by using the measured attitudes of the fault plane and the slip axis, and by substituting friction coefficients of 0.0 to 2.0. This formulation generates an overdetermined linear system which is solved for the stress tensor (σ_i) once for each friction coefficient.

The quality of a solution is evaluated by comparing the orientations of the principal axes of two stress tensors. The first tensor, σ_i, can cause slip on the entire fault cluster (Reches, 1987). This tensor is common to all faults in the cluster and is viewed as a "mean" tensor. The second tensor, $[S_i]_j$, is calculated for the j_{th} fault in the cluster. It can cause slip on the j_{th} fault for the minimum value of the shear stress $(S_1)S_3)/2$. In other words, $[S_i]_j$ is the tensor which cause yielding of the j_{th} under the Mohr–Anderson yield condition. The mean angle between the two tensors is:

$$T_m = \left[\Sigma(\sigma_i \hat{} S_i)_j\right]/3N,\ j = 1 \text{ to } N,\ i = 1, 2, 3$$

where N is the number of faults in the cluster. T_m is defined as the misfit angle of the principal axes (Reches et al., 1989) and varies from 0° to 90°. The solution with the smallest T_m is considered the best solution for the cluster. Faults with large misfit angles or faults for which the predicted sense of slip is opposite to the observed sense are rejected (Reches, 1987). If $T_m \geq 45°$, the cluster probably contains faults which slipped during more than one tectonic phase. This cluster can be separated into two subclusters according to the misfit angles (Baer and Reches, 1989).

Results

For each station the stress inversion was performed for two attitudes of the faults: the current attitude in the field, and the attitude of the faults after retilting the host layers to the horizontal (by rotation around the strike). The solutions for the

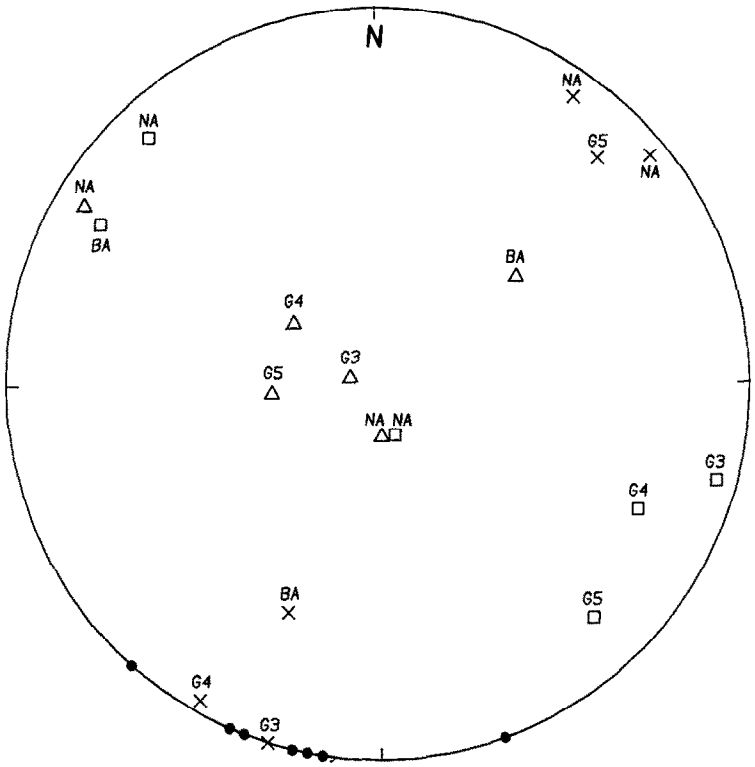

Fig. 4. Composite stereoplot of stress solutions and basaltic dikes in the Gilboa'. The diagram includes (1) the principal axes of the six clusters (σ_1 as boxes, σ_2 as triangles, σ_3 as crosses), and (2) poles to dikes (dots). Cluster symbols are *G3*, *G4* and *G5* for Gid'ona quarry levels 3, 4 and 5, *BA* for Bet-Alfa quarry, and *NA* for Nahal Avinadav quarry (two clusters). Lower hemisphere, equal-area projection.

retilted faults appear to be better than the solutions for the non-retilted faults: The retilted faults have smaller standard deviations, and the determined stress tensors of the retilted faults at different stations are more similar to each other than the corresponding non-retilted stress tensors. Further, the determined principal stress axes of the retilted faults are closer to verticality and horizontality than those of the non-retilted ones, as expected for a tectonic stress field (Baer and Reches, 1989). These observations indicate that the small faults slipped before the tilting of the host layers (Reches, 1976).

Valid stress solutions were obtained for all five stations: it was necessary to reject only five out of 96 faults. Figure 3 and Table 1 show the field data, the stress tensors of the best solutions, and the confidence margins of the solutions (Reches, 1987). Six clusters are shown because the Nahal Avinadav data were split into two subclusters. The two subclusters of normal faults and strike-slip faults are displayed as (e) and (f) in Table 1 and Fig. 3. Figure 4 is a summary projection of the stress tensors of the six clusters and the dikes of the Gilboa'.

The state of stress of strike-slip faulting implies that $\sigma_H > \sigma_v > \sigma_h$, where σ_H and σ_h are the maximum and minimum horizontal compression axes, and σ_v is the vertical stress. Five out of the six clusters in the Gilboa' exhibit such stress. Clusters (a)–(e) in Fig. 3 and Table 1 indicate that σ_1 and σ_3 are generally subhorizontal ($\sigma_1 \approx \sigma_H$ and $\sigma_3 \approx \sigma_h$) and σ_2 is subvertical ($\sigma_2 \approx \sigma_v$). The stress ratio ϕ is approximately 0.5 (Table 1), where $\phi = \sigma_2 - \sigma_3/\sigma_1 - \sigma_3$, which is typical for strike-slip conditions. The stress axes of these clusters have generally similar orientations, the σ_1 axes trending between 106° and 138°, and the σ_3 axes trending between 16° and 49° (Fig. 3). The angular variations of these axes do not reflect spatial variations (e.g., the three stations in Gid'ona quarry display about the same angular variations as the entire Gilboa' block (Fig. 4).

It appears that the five clusters represent a

single state of stress, defined here as the "Gilboa' Stress". The means of the principal axes of the five clusters are regarded as comprising the Gilboa' Stress Tensor. The mean directions and standard deviations are as follows: σ_1 axis, $3.4°/123.6° \pm 12.3°$; σ_2 axis, $89.9°/289° \pm 23°$; and σ_3 axis, $3.2°/211.2° \pm 12.8°$. The stress ratio is $\phi = 0.58 \pm 0.09$ (Fig. 4). For simplicity, we ignore the few degrees of plunge of the σ_1 and σ_3 axes, and consider them as horizontal toward 122° and 32° respectively.

The stress tensor for the cluster of normal faults in Nahal Avinadav (Fig. 3f) differs from the Gilboa' Stress (Fig. 4). Both tensors share the same orientation of σ_3, but the normal faults in Nahal Avinadav have subvertical σ_1 axes, subhorizontal σ_2 axes and $\phi = 0.07$.

Discussion

Neogene dikes, uplift and the age of the Gilboa' Stress

Hatzor (1988) mapped nine dikes composed of olivine alkali basalt at six sites along the Gilboa' margins (Fig. 2). Five of the dikes are fresh and were traced on areal photographs; these dikes trend between 280° and 290° in the northern and eastern Gilboa'. The other four dikes are altered and poorly exposed; they trend 250° (two dikes), 280° and 310°. Two of the fresh dikes were dated by the K–Ar method by Shaliv and Steinitz (1988). The first age of 4.7 ± 0.13 Ma is for one out of two dikes which trend 290° in Nahal Avinadav, eastern Gilboa' (Fig. 2). The second age of 10.3 ± 0.2 Ma is for one out of three dikes which trend 280°, in Hefzi-Bah quarry in northern Gilboa' (Fig. 2).

The extension associated with the emplacement of a dike is clearly normal to it. Thus, the fresh dikes in the Gilboa' indicate subhorizontal extension in the 10°–20° direction. This extension axis agrees, in general, with the trend of σ_3 of the Gilboa' Stress, which is $32° \pm 12°$ (Fig. 4). Therefore, we infer that the Gilboa' Stress Field prevailed during Miocene–Pliocene times, the period of emplacement of the dikes.

Igneous bodies also reveal the time of uplift of the Gilboa' block along the Gilboa' fault on the northern side and along the Dead Sea marginal faults on the eastern side (Fig. 2) (Hatzor, 1988). Both fault systems are active and from prominent morphological escarpment zones. Based on the following observations the uplift of the Gilboa' is not older then 5.9 Ma: First, a 10.3 Ma old intrusion in Hefzi-Bah quarry (Fig. 2) and a 5.2 Ma old basalt flow west of Gid'ona were both downfaulted along the Gilboa' fault (Fig. 2)(ages after Shaliv and Steinitz, 1988). Second, Hatzor (1988) found an erosional surface at an elevation of 400 m on top of the Gilboa' block which truncates two basalt fields; these fields are 17 and 5.9 Ma old according to Shaliv and Steinitz (1988). The erosional surface is locally covered by well-rounded, large pebbles, which suggests that it was formed at low elevations. Thus, Hatzor (1988) concluded that the Gilboa' region was uplifted after 5.9 Ma, after the development of the erosional surface on the top of the Gilboa' block. The uplift of the Gilboa' block was either contemporaneous with or followed the period of the Gilboa' Stress.

The Gilboa' Stress derived by the stress inversion of the small faults fits the trend of the basaltic dikes (Fig. 4). Further, even the separate cluster of normal faults in Nahal Avinadav (Fig. 3f), has the same extension axis as the Gilboa' Stress. A similar situation, in which σ_3 maintains a constant trend while σ_1 and σ_2 interchange positions, occurs today in the western parts of the Basin and Range (Zoback and Zoback, 1980).

The simple patterns of the small faults which have been examined and the similarity of the calculated stress tensors leads us to conclude that the Gilboa' block was subjected to *a single and uniform state of stress*. This began no later than Middle Miocene (10.2 Ma date for a dike trending 280°) and continued to act at least during the early Pliocene (4.7 Ma date for the dike trending 290°). As only one stress state was detected here, and as the Gilboa' region was active after the Pliocene (Hatzor, 1988), we believe that the Gilboa' Stress may also be active today.

The Gilboa' Stress and regional stress fields

The tectonic paleostresses in the Sinai–Israel subplate were determined in previous analyses of

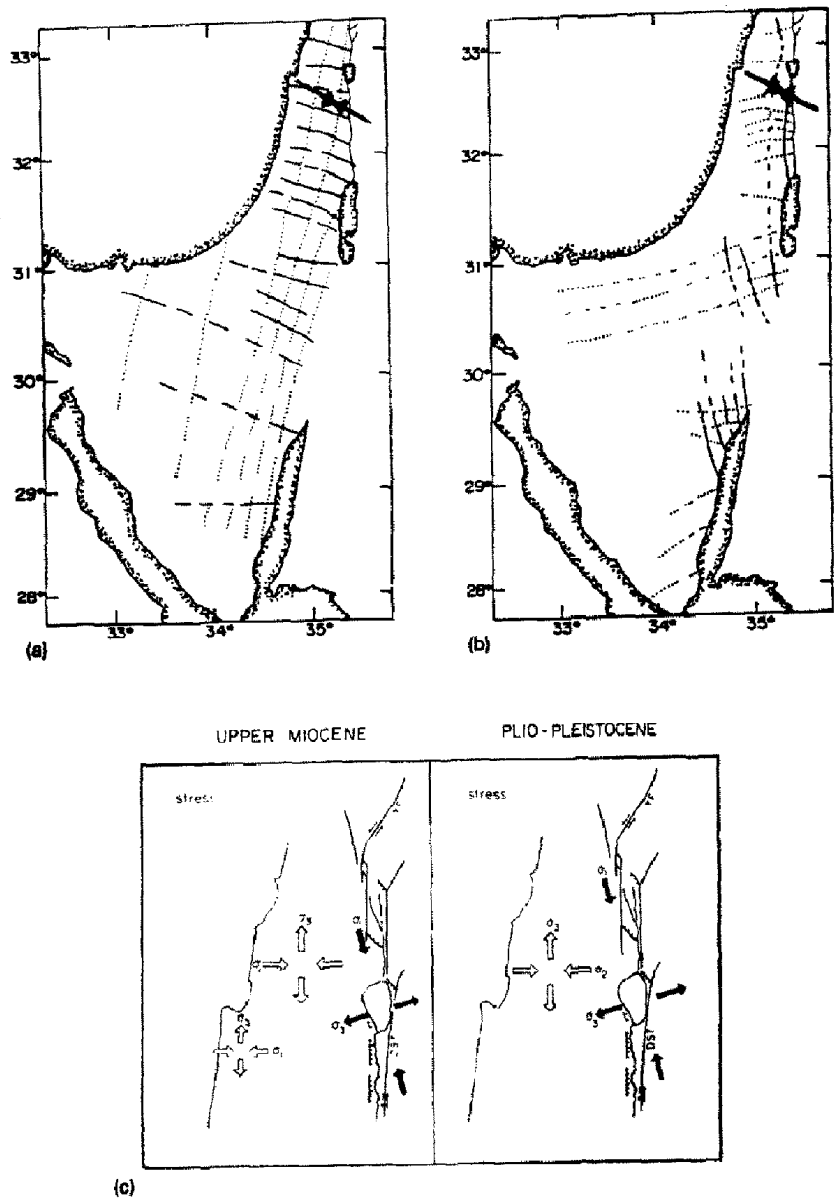

Fig. 5. Regional tectonic paleostress fields in the Sinai–Israel subplate. The Syrian Arc Stress (a) and the Dead Sea Stress (b) (after Eyal and Reches, 1983). σ_H trajectories are continuous lines; σ_h trajectories are dotted lines; σ_H of the Gilboa' Stress is marked with heavy arrows. c. The paleostresses in northern Israel; open arrows indicate the stresses within the subplate and solid arrows indicate the stresses within the Dead Sea transform zone (after Ron and Eyal, 1985). *DST*—Dead Sea transform; *YF*—Yammuneh Fault.

small structures (Letouzey and Tremolieres, 1980; Eyal and Reches, 1983). Eyal and Reches (1983) recognized two regional stress fields (Fig. 5): (1) the Late Cretaceous to Neogene Syrian Arc Stress (SAS), with σ_H, the axis of maximum horizontal compression, trending between E–W and WNW–ESE, and (2) the Neogene to Recent Dead Sea Stress (DSS), with σ_h, the axis of least horizontal compression, trending between WSW–ENE and E–W. Ron and Eyal (1985) determined geographically restricted stress fields in northern Israel (Fig. 5). In the Galilee, the prevailing stresses were E–W compression during the Late Miocene to early Pliocene and N–S extension in the post-middle Pliocene period. Since the Early Miocene (Fig. 5c), the prevailing stresses in the Dead Sea rift, 30 km east of the central Galilee, were NNW–SSE compression. In terms of stress trends and char-

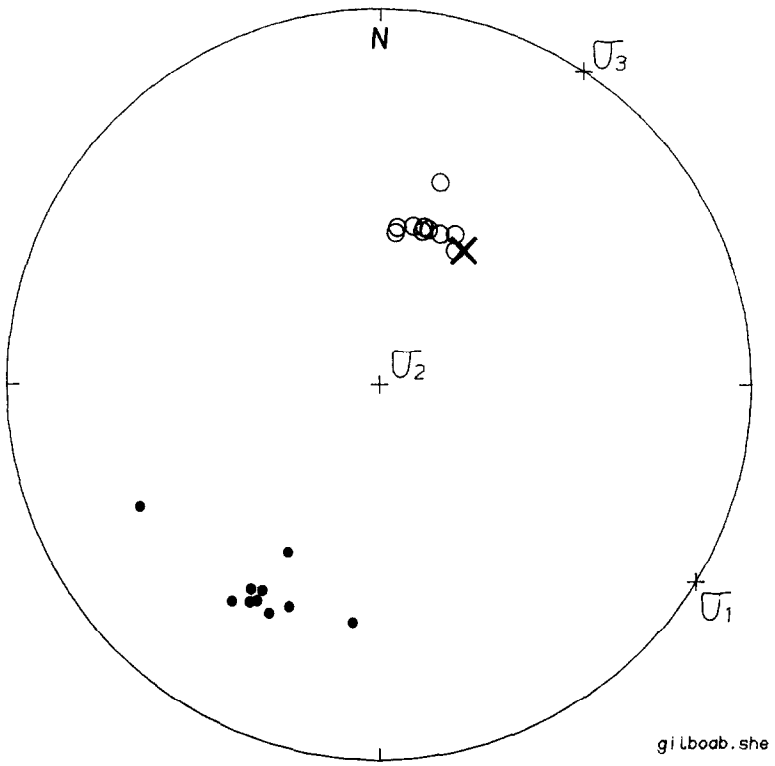

Fig. 6. Stereoplot of the Gilboa' fault plane data and shear stress. Poles to measured fault planes (dots); measured slip axes (circles); the Gilboa' Stress tensor (sigma symbols); the calculated axis of maximum resolved shear stress (heavy cross). Lower hemisphere, equal-area projection.

acter, the Gilboa' Stress fits well to the SAS. The Gilboa' Stress was, however, active during the early Pliocene, and it may still be active even today. Thus, the present study indicates that stresses which have a trend similar to that of the SAS were active beyond the time span suggested for the duration of the SAS by Eyal and Reches (1983). This longer duration is no surprise. Mimran (1984) showed that Neogene sediments are tilted by up to 37° along the eastern flank of the Faria articline (Fig. 1); Pliocene or younger folding being responsible for this structure. Ron and Eyal (1985) showed that E–W compression and N–S extension (generally compatible with the SAS) were active in northern Israel, away from the Dead Sea rift, during the Late Miocene to early Pliocene.

Shear stresses along the regional fault systems

The Dead Sea transform and the Carmel–Gilboa' fault, which bound the Gilboa', were active during the Pliocene to Recent period, and the activity of the Gilboa' Stress tensor during the Pliocene (to Recent?), prompts a few interesting questions, which are discussed below.

Slip along the Gilboa' fault

The Carmel–Gilboa' zone, which forms the southern margins of the Yizre'el depression (Figs. 1 and 2), has been regarded as a left-lateral wrench fault or a normal fault (see above). The Gilboa' fault is composed of interconnected segments which form a zig-zag fault with a general WNW–ESE trend (Fig. 2). We attempt here to derive the expected slip direction along the Gilboa' fault when it is subjected to the Gilboa' Stress. For these calculations we selected a zone of a few hundred meters in length close to Hefzi-Bah (Fig. 2); the slickenside fault surface is exposed at many sites along this zone. The strike of this zone is 120°, subparallel to the general trend of the Gilboa' fault. We measured the fault attitude at ten sites along this exposure. The mean fault dip is 55°/030° ± 5°, and the mean plunge of the

slickenside striations, which were measured independently, is 53°/016° ± 5° (Fig. 6); these orientations indicate normal slip with a small left-lateral component.

We assume that the slip along the fault occurred in the direction of maximum resolved shear stress (following Bott, 1959). Then the principal stress axes of the Gilboa' Stress (σ_1 at 0°/122°, σ_2 vertical and σ_3 at 0°/032°) (see Fig. 6) are substituted into the mean attitude of the Gilboa' fault plane by using the formulations of Jaeger and Cook (1979, Chap. 2). The derived axis of maximum resolved shear stress is 54°/040°, deviating by only 14.7° from the mean axis of the observed slickenside striations (Fig. 6).

It may at first be surprising that the normal slip along the Gilboa' fault is compatible with the Gilboa' Stress, indicating strike-slip conditions. This result stems form the parallelism between the strike of the Gilboa' fault and the σ_1 axis of the Gilboa' Stress (Fig. 6). Due to this parallelism, σ_1 has a negligible influence on the shear stress along the major fault and the direction of the maximum resolved shear.

The above analysis indicates that two strain modes have been active in the northern Gilboa' since the Neogene: the block is internally deformed by small strike-slip faults (Fig. 3), whereas the major Gilboa' fault is a normal fault (Fig. 6). The axis of least compression is the same for the small faults and the Gilboa' fault but their maximum compression axes have different trends.

Stress rotation associated with the Dead Sea transform

Eyal and Reches (1983) found that the Dead Sea Stress (DSS) in the Sinai–Israel subplate is characterized by σ_h trending WSW–ENE to E–W (Fig. 5b). The DSS is compatible with the left-lateral slip and extension along the leaky Dead Sea transform. The σ_H of the SAS trends 60° to 90° from the Dead Sea trend, and it generates negligible shear along the Dead Sea fault and increases the normal stress across it. Thus, one expects that the SAS has not been active since the Middle Miocene (Eyal and Reches, 1983), the period of activity along the Dead Sea transform (Garfunkel, 1981).

The Gilboa' Stress, which is similar in trend to the SAS, has been active at least during the Miocene and early Pliocene (and most likely later). How could the SAS cause left-lateral slip and extension along the N–S trending Dead Sea transform? Part of the solution was signaled by Eyal and Reches (1983) and Ron and Eyal (1985) who noted that the stress field *within* the Dead Sea rift may differ from the stress field *away* from it (Fig. 5c). Eyal and Reches (1983) noticed that evidence for the DSS is concentrated primarily within the Dead Sea rift. Ron and Eyal (1985) found that the prevailing paleostresses in the Galilee (northern Israel) were E–W compression during the Late Miocene to early Pliocene and N–S extension during the post-middle Pliocene period (Fig. 5c). In contrast, the prevailing stresses within the 20–30 km wide zone of the Dead Sea transform, east of the Galilee (Fig. 1), were NNW–SSE compression since the Early Miocene.

From these observations, it could be possible that the SAS was active in the Sinai–Israel subplate even during the Neogene, but that it was *rotated* in the proximity of the Dead Sea transform zone. In the case of the Gilboa' region, a clockwise rotation of about 40° would generate a stress state similar to the DSS in the Dead Sea rift east of the Gilboa'.

Stress rotation on a larger scale has been proposed for the San Andreas fault in central California. Zoback et al. (1987) compiled a stress map based on in-situ stress measurements, focal plane solutions and young structures. Their stress map indicates that σ_H generally trends subperpendicular to the San Andreas fault within a 200 km wide domain on both sides of the fault. The orientation of σ_H in this domain deviates by 45°–60° from the orientation predicted by the Anderson theory. Zoback et al. (1987) proposed that this large angular deviation indicates rotation of the regional stress field in the proximity of a weak San Andreas fault.

Whether the stress rotations proposed for the Dead Sea and the San Andreas transform faults reflect similar mechanisms is unknown, but we believe that both rotations indicate the effects of the mechanical properties of a transform zone on the regional stress field.

Conclusions

The Gilboa' block is internally folded into NNE–SSW folds and flexures, and bounded by the normal faults of the Carmel–Gilboa' system in the north and by the faults of the Dead Sea system in the east. All these elements have been active at least since the Miocene.

The tectonic paleostresses in the Gilboa' were determined from small faults and basaltic dikes. We have found that a single state of stress dominated the Gilboa' since the Miocene. The means of the directions of the principal axes and their standard deviations are: σ_1, $3°/12° \pm 12°$; σ_2, $90° \pm 23°$; and σ_3, $3°/211° \pm 13°$. This stress field fits well with the trends of the Syrian Arc folds in the Gilboa' and is compatible with normal slip along the Gilboa' fault. As this stress is incompatible with the either left-lateral slip or normal faulting along the Dead Sea system, we suggest that stress rotation may have occurred within the Dead Sea rift.

Acknowledgements

The discussions with Y. Mimran, G. Baer and G. Shaliv of the Geological Survey of Israel and A. Starinsky of the Hebrew University, contributed significantly to our understanding of the structure of the Gilboa'. Gidon Baer reviewed the manuscript and helped in the preparation of the figures. The study was in part supported by the US–Israel Binational Science Foundation (grant 86-183).

References

Baer, G. and Reches, Z., 1989. Tectonic stresses, igneous intrusions and structural development of two domes in Ramon, southern Israel. Tectonophysics, 166: 293–315.

Bartov, Y., Steinitz, G., Eyal, M. and Eyal Y., 1980. Sinistral movement along the Gulf of Aqaba—its age and relation to the opening of the Red Sea: Nature, 285: 220–222.

Ben Avraham, Z. and Hall, J.K., 1977. Geophysical survey of Mount Carmel structure and its extension into the eastern Mediterranean. J. Geophys. Res., 82: 793–802.

Bott, M.H.P., 1959. The mechanics of oblique slip faulting. Geol. Mag.., 96: 109–117.

De Sitter, L.U., 1962. Structural development of the Arabian Shield in Palestine. Geol. Mijnbouw, 41 (3): 116–124.

Eyal, Y. and Reches, Z., 1983. Tectonic analysis of the Dead Sea Rift region since Late Cretaceous based on mesostructures. Tectonics, 2 (2): 167–185.

Freund, R., 1965. A model of the structural development of Israel and adjacent areas since Upper Cretaceous times. Geol. Mag., 102: 189–205.

Freund, R., 1970. The geometry of faulting in the Galilee. Isr. J. Earth Sci., 19: 117–140.

Garfunkel, Z., 1981. Internal structure of the Dead Sea leaky transform (rift) in relation to plate kinematics: tectonophysics, 80: 81–108.

Hatzor, Y., 1988. The geology of the Gilboa' region. M.Sc. Thesis, Hebrew Univ., Jerusalem (Unpubl.) (in Hebrew with English Abstr.).

Jaeger, J.C. and Cook, N.E.W., 1979. Fundamentals of Rock Mechanics. Chapman and Hall, London, 3rd ed.

Letouzey, J. and Tremolieres, P., 1980. Paleostress around the Mediterranean since the Mesozoic from microtectonics: Comparison with plate tectonic data. Rock Mech., 9: 173–192.

Mimran, Y., 1984. Unconformities on the eastern flank of the Faria Anticline, and their implications for the structural evolution of Samaria (Central Israel). Isr. J. Earth Sci., 33: 1–11.

Neev, D., 1975. Tectonic evolution of the Middle East and the Levantine Basin (easternmost Mediterranean). geology, 3: 683–686.

Reches, Z., 1976. Analysis of joints in two monoclines in Israel. Geol. Soc. Am. Bull., 87: 1654–1662.

Reches, Z., 1983. Faulting of rocks in three dimensional strain fields, II. Theoretical analysis. Tectonophysics, 95: 133–156.

Reches, Z., 1987. Determination of the tectonic stress tensor from slip along faults that obey the Coulomb Yield Criterion. Tectonics, 6: 849–861.

Reches, Z., Baer, G. and Hatzor, Y., 1989. Stress inversion of fault slip data and focal plane solutions—the method and its applications to tectonic analysis. Isr. Geol. Soc. Annu. Meet., p. 129 (Abstr.).

Ron, H. and Eyal, Y., 1985. Intraplate deformation by block rotation and mesostructures along the Dead Sea transform, northern Israel. Tectonics, 4: 85–105.

Schulmann, N. and Bartov, Y., 1978. Tectonics and sedimentation along the Rift Valley. Int. Assoc. Sedimentol. Guideb., Part 2, pp. 37–94.

Shaliv, G. and Steinitz, G., 1988. K–Ar of Lower Basalt, Intermediate Basalt and base of Cover Basalt in northern Israel. Geol. Surv. Isr. Curr. Res., 6: 22–28.

Zoback, M.L. and Zoback, M., 1980. State of stress in the conterminous United States. J. Geophys. Res., 85: 6113–6156.

Zoback, M.D., Zoback, M.L., Mount, V.S., Suppe, J., Eaton, J.P., Healy, J.H., Oppenheimer, D., Reasenberg, P., Jones, L., Raleigh, C.B., Wong, I.G., Scotti, O. and Wentworth, C., 1987. New evidence on the state of stress of the San Andreas Fault System. Science, 238: 1105–1111.